Letter

Effect of receptor clustering on chemotactic performance of *E. coli*: Sensing versus adaptation

Shobhan Dev Mandal and Sakuntala Chatterjee
Department of Theoretical Sciences, S. N. Bose National Centre for Basic Sciences, Block JD, Sector 3, Salt Lake, Kolkata 700106, India

(Received 10 August 2020; accepted 5 February 2021; published 2 March 2021)

We show how the competition between sensing and adaptation can result in a performance peak in *Escherichia coli* chemotaxis using extensive numerical simulations in a detailed theoretical model. Receptor clustering amplifies the input signal coming from ligand binding which enhances chemotactic efficiency. But large clusters also induce large fluctuations in total activity since the number of clusters goes down. The activity and hence the run-tumble motility now gets controlled by methylation levels which are part of adaptation module rather than ligand binding. This reduces chemotactic efficiency.

DOI: 10.1103/PhysRevE.103.L030401

I. INTRODUCTION

With the advent of sophisticated techniques to measure single-cell response in experiments [1,2], an important question has emerged: how behavior of a cell is affected by the fluctuations present in the intracellular biochemical reaction network [3–6]. In this paper we address this question for *Escherichia coli* chemotaxis, one of the best characterized systems in biology [7].

The chemotaxis describes the migration tendency of the *E. coli* cell towards the region of higher nutrient concentration. The underlying biochemical network has two main modules, sensing and adaptation, which are coupled to each other through the activity of the transmembrane chemoreceptors. The receptor activity changes with binding of the receptor to the nutrient ligand molecules and with methylation. There are a few thousand receptors in a cell, and they show strong cooperativity where the neighboring receptors form clusters or "teams" and switch between active and inactive states in unison. This helps in amplification of the input signal coming from ligand binding and allows the cell to respond to even a weak gradient of nutrient concentration [8–10].

In recent experiments involving single-cell FRET measurements it was observed that receptor clustering results in surprisingly large activity fluctuations inside a cell [11,12] even in the absence of methylation noise. This observation was striking since methylation was long believed to be the most important source of noise in a chemotaxis network [13–17]. The experiments in Refs. [11,12] showed that receptor clustering is an independent and equally important noise source in the pathway. The immediate and important question here is how this newly found noise source is related to the chemotactic performance of the cell.

In this work, we address this question within a detailed theoretical model and find that there is an optimum size of the receptor cluster at which the chemotactic performance is at its best. Since receptor clustering amplifies the input signal coming from ligand binding, it is expected to enhance the cell performance [8–10]. However, when clusters become significantly large, the total number of clusters goes down proportionately. The total activity of the cell, which is the sum of activity of all the clusters, starts showing large fluctuations since the sum is now performed over a small number of signaling teams (also see Sec. 3 of Ref. [18]). When the activity gets too high or too low, the adaptation comes into play and the receptor methylation level undergoes large change to restore the activity to its mean value. Our data show that the total activity which controls the run-and-tumble motility of the cell is guided by methylation rather than ligand binding for large receptor clusters. This reduces the chemotactic efficiency of the cell, and its performance goes down.

Our study brings out a fundamentally important point: how competition between sensing and adaptation may result in a performance peak. We demonstrate this by monitoring several different quantities as measures of performance. In the presence of a spatially varying nutrient concentration profile we define a good chemotactic performance by measuring how fast the cell is able to climb up the gradient, or how strongly it is able to localize itself in the nutrient-rich regions [16,19]. A good performance implies a strong ability of the cell to distinguish between regions with high and low nutrient concentration. We find that for an optimal size of the receptor cluster this ability is most pronounced. Interestingly, our conclusion remains valid even when the cell is tethered and is not moving around using run-tumble motility. In this case we define the performance by the differential response of the cell when the nutrient level at its location is increased or decreased. The rotational bias of the flagellar motors shows maximum difference between the ramped up and ramped down inputs at a specific size of the receptor cluster.

II. MODEL

In an *E. coli* cell the chemoreceptors pair up to form homodimers, and three such homodimers form a trimer of dimers (TD) [20,21]. In our description, a signaling team of size n contains n number of TDs. The free energy difference (in units of K_BT) between the active and inactive states of a dimer is calculated according to Monod-Wyman-Changeux

 ©2021 American Physical Society

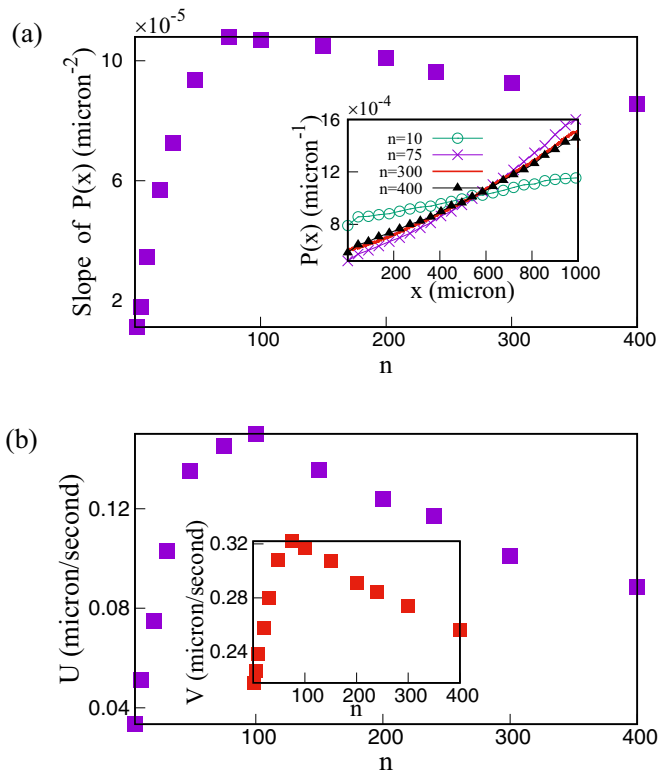

FIG. 1. Peak in localization and drift velocity as a function of receptor cluster size. (a) The x-position distribution of the cell shows steepest variation at an optimum n. Inset shows form of $P(x)$ for few representative n values. (b) Chemotactic drift velocity measured from net displacement in a run (inset) and net displacement in a fixed time interval $T = 40$ s (main plot); both show a peak for a specific n. We have used a linearly varying nutrient concentration profile here. Each data point has been averaged over at least 10^7 histories. The simulation parameters are given in Table S1 in Ref. [18].

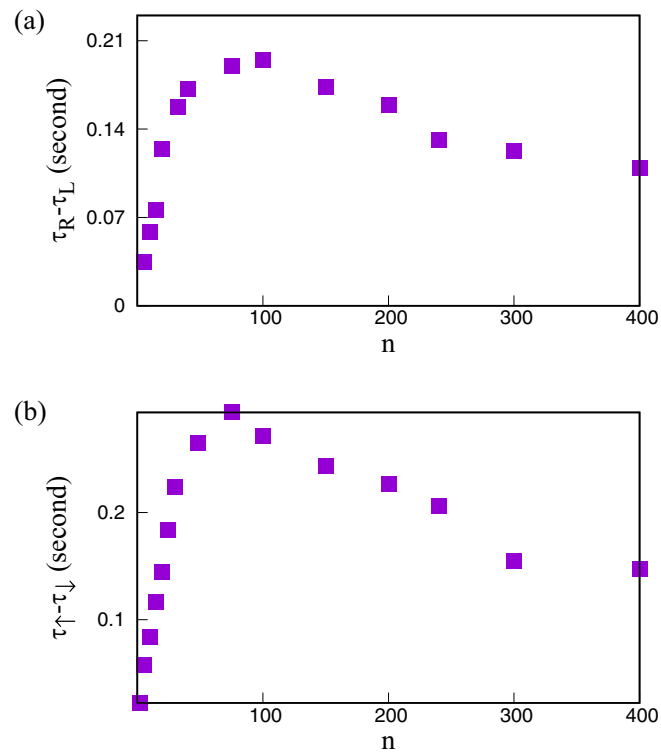

FIG. 2. Motor response of the cell shows highest sensitivity at a specific size of receptor cluster. (a) For a swimming cell, the mean first passage time to the tumble mode for uphill run (τ_R) and downhill run (τ_L) shows the largest difference at a particular n. (b) For a tethered cell in CCW mode, the mean first passage time to CW mode when the nutrient level is ramped up ($\tau_\uparrow$) and ramped down ($\tau_\downarrow$) at a rate 0.1 μM/s shows the largest difference at a specific n. All data have been averaged over at least 10^6 histories. The simulation parameters are as in Fig. 1.

model [22–24]:

$$\epsilon[m, c(x)] = 1 + \log \frac{1 + c(x)/K_{\min}}{1 + c(x)/K_{\max}} - m, \qquad (1)$$

where $c(x)$ is the nutrient concentration at the cell location x and m is the methylation level of the dimer which can take integer values between 0 and 8. The constants $K_{\min}$ and $K_{\max}$ set the range within which a chemical concentration can be sensed by the cell. The total free energy of the cluster is the sum of free energy of the individual dimers. All dimers in a cluster change their activity states simultaneously, and the transition probability depends on the cluster free energy [18].

The methylation level of a dimer is controlled by methylating enzyme CheR and demethylating enzyme CheB-P. A dimer can bind to one enzyme molecule at a time. An inactive dimer gets methylated by CheR, and the probability to find it in active state increases. On the other hand, an active dimer gets demethylated by CheB-P, and its activity decreases. Unphosphorylated CheB receives its phosphate group from autophosphorylation of active receptors. This constitutes a negative feedback in the reaction network and is responsible for adaptation. Autophosphorylation of active receptors also supplies phosphate group to another protein CheY, and the resulting CheY-P binds to the flagellar motors and induces tumbling in the cell motion. A high value of total activity implies large tumbling probability.

However, the number of enzyme molecules is far too low compared to the number of dimers in a cell [25], and it takes a long time for a dimer to bind to an unbound enzyme molecule in cell cytoplasm [26]. To reconcile the low abundance of enzyme molecules with near-perfect adaptation of the cell [27,28], few mechanisms like "brachiation" or "assistance neighborhood" have been proposed [29–31] and experimentally verified [32,33] which allow a single bound enzyme to modify the methylation level of more than one dimers before it unbinds and returns to the cell cytoplasm [23,31,34]. We include a flavor of this mechanism in our model. A complete description of our model and other simulation details can be found in Ref. [18]. We perform Monte Carlo simulations on this model in one and two spatial dimensions. We present the data for two dimensions below and include those for one dimension in Ref. [18].

III. PERFORMANCE PEAK AT AN OPTIMAL SIZE OF RECEPTOR CLUSTER

For a swimming cell with a linearly varying $c(x)$, the steady-state position distribution $P(x)$ of the cell also assumes

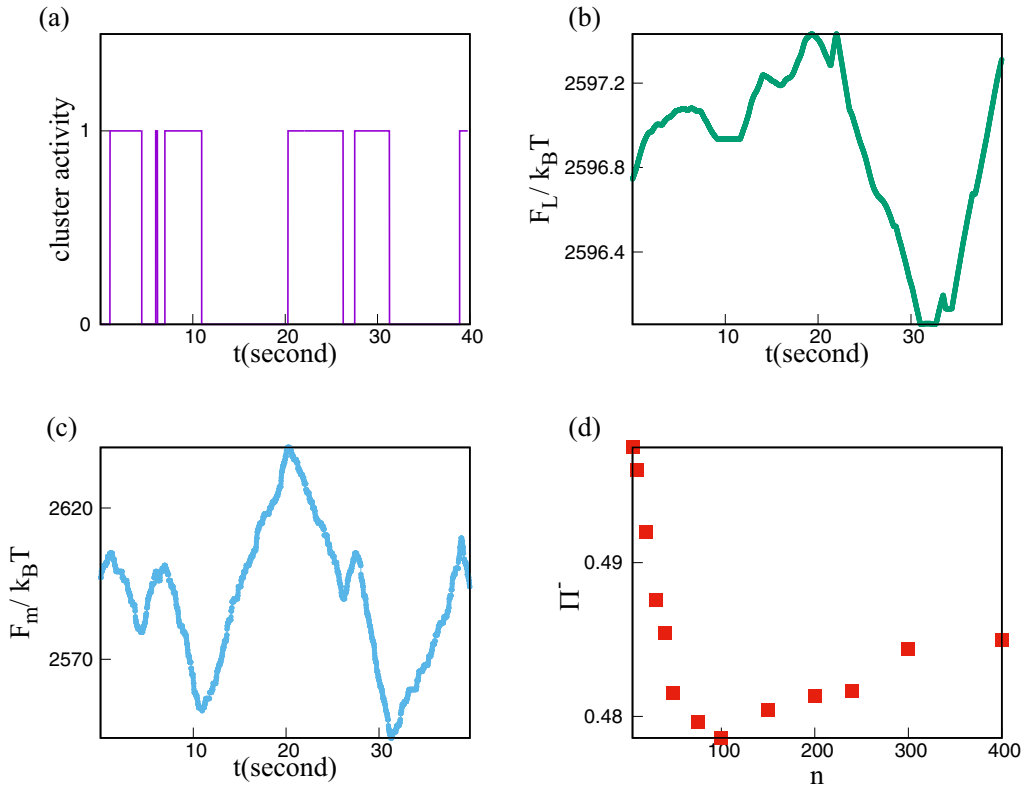

FIG. 3. Typical time series of activity along with methylation component and ligand component of free energy of a receptor cluster of size $n = 200$. The time series has been recorded in steady state over a time window of 40 s. (a) A few transitions of activity state of the cluster. (b) Simultaneous variation of free energy (in unit of $k_B T$) due to ligand binding, which directly captures the run-tumble trajectory of the cell. (c) Variation of methylation free energy (in unit of $k_B T$) of the cluster, which is seen to roughly follow the activity transitions. The scale of variation of ligand binding energy is negligible compared to that of methylation for the present value of n. (d) Probability Π^- that in a time interval $T = 40$ s the net displacement of the cell is negative, shows a minimum, and then increases for large n. The simulation parameters used are same as those in the Fig. 1(b) main plot.

an almost linear form [see inset of Fig. 1(a)]. Clearly, a good performance implies a steep slope of $P(x)$. In Fig. 1(a) (main plot) we plot this slope as a function of receptor cluster size and find a peak. A related quantity $\langle C \rangle = \int P(x)c(x)\,dx$ which gives the average nutrient amount experienced by the cell is often used to characterize performance when $c(x)$ or $P(x)$ is not linear [15,16,35]. We find a similar peak in $\langle C \rangle$ also (data not shown here). Chemotactic drift velocity V measures how fast the cell climbs up the concentration gradient, and a large V implies a good performance. To extract V from the run-and-tumble trajectory of the cell we measure the mean value of net displacement of the cell in a run and divide it by the mean run duration [16,36–39]. We present our data in Fig. 1(b) inset, which shows a pronounced peak. Another possible way to measure the drift velocity is from the net displacement in a fixed time interval T and divide that by T. In the main plot of Fig. 1(b) we show the plot for this quantity, denoted as U, and find a similar peak.

At the core of chemotactic sensing lies the differential behavior of the cell when the nutrient level in its environment goes up or down. This difference should be large for a good performance. When a cell is running in the direction of increasing nutrient concentration, its tumbling rate decreases and the run is extended. Similarly, for a run towards a lower nutrient level, the tumbling rate increases and the run is shortened. We measure the time till the first tumble during an uphill run and a downhill run and plot their difference in Fig. 2(a). This difference shows a peak at a specific size of the receptor cluster. Interestingly, we can use a similar measure to quantify performance for a tethered cell as well, which is more commonly used in experiments. In this case we apply a nutrient concentration that is increasing (decreasing) linearly with time while the flagellar motors are rotating in the counterclockwise (CCW) direction. We measure the average time till the transition to clockwise (CW) rotation mode. In order to compare with the swimming cell, we change the nutrient level at the same rate as that experienced by a swimming cell during a run. We plot the difference between ramped up and ramped down cases in Fig 2(b) and find a peak at the optimal cluster size.

From our data in Figs. 1 and 2 it follows that for various different performance criteria, the single-cell chemotaxis shows optimality. The position of the performance peak may slightly vary depending on the specific measure we use to quantify performance, as seen in the above plots. But the most striking feature here is the existence of a peak at some value of n. Below we explain the origin behind this effect.

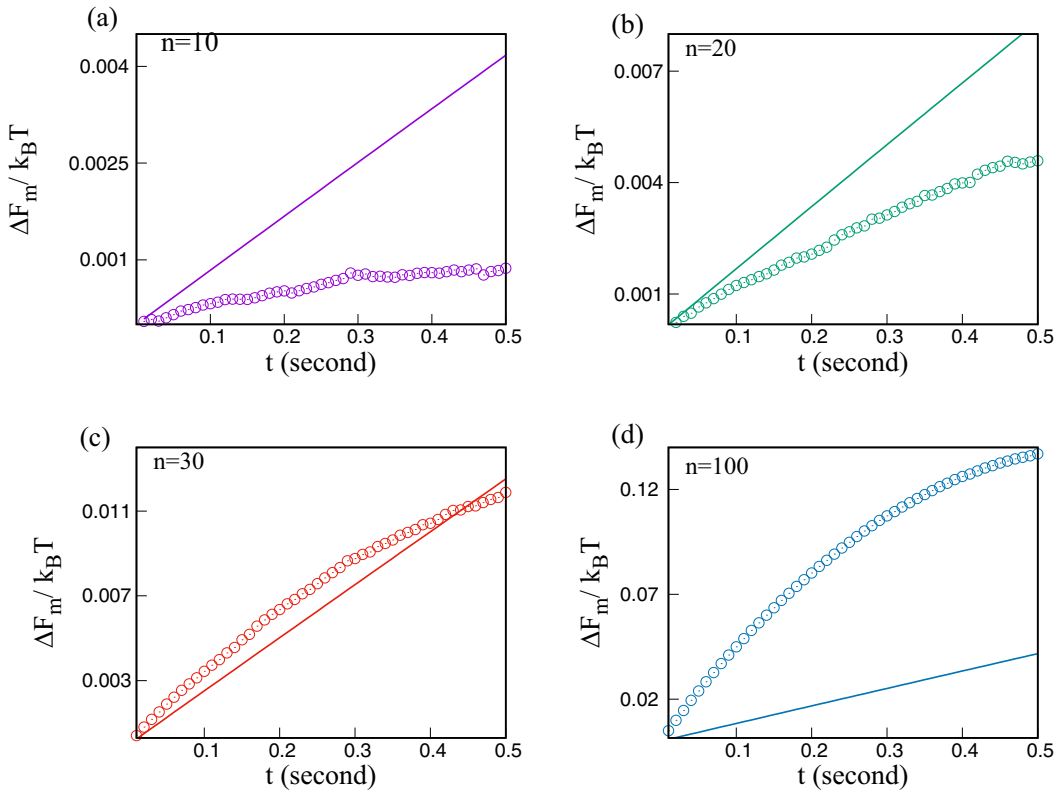

FIG. 4. Average change ΔF_m (in unit of k_BT) in methylation free energy (discrete points) of a cluster for first 0.5 s during an uphill run for four different n values. The continuous lines show the change in ligand free energy (in unit of k_BT) of the cluster. For small n the change in ligand free energy dominates, but as n increases, ΔF_m takes over. These data have been averaged over at least 2×10^6 histories.

IV. COMPETITION BETWEEN SENSING AND ADAPTATION

The probability to find a receptor cluster in the active state is $[1 + \exp(F_L - F_m)]^{-1}$, where F_L is the sum of ligand binding energy of all dimers in the cluster and F_m is the total methylation of all those dimers. Since the contribution due to ligand binding is the same for all dimers, F_L is proportional to n. As the cell swims up (down) the ligand concentration gradient, F_L increases (decreases) with time [see Eq. (1)], and this change is proportionately larger with n. This means as n increases, the activity of a receptor cluster decreases (increases) quickly during an uphill (downhill) run, thereby elongating (shortening) the run, since activity controls the tumbling rate (see model details in Ref. [18]). This is why the chemotactic performance gets better with n. For large n, however, the number of clusters is less, and the activity, which is calculated by averaging over all clusters, now shows large fluctuations. Switching the activity state of one large cluster brings about a large change in the total activity of the cell. For example, when the activity gets too low, all the inactive dimers in a cluster tend to get methylated. This increases F_m significantly, and the change in F_m overrides the change in F_L. See Fig. 3 for a typical time series of cluster activity, F_m and F_L for a large n value. In Fig. 4 we plot the average change ΔF_m in methylation free energy as a function of time during an uphill run of the cell for various different n. The change in F_L has been shown with a continuous line for reference. These plots clearly show for large n the change in F_m overtakes the change in F_L. The variation in cluster free energy is then controlled by F_m. The cell is now less sensitive to the ligand concentration profile. A shorter uphill run and a longer downhill run now become increasingly likely. In Fig. 3(d) we plot the probability to find a negative net displacement of the cell during a time interval T, and indeed after reaching a minimum this probability increases again for large n. This reduces the value of the chemotactic drift velocity and brings down the performance when n is large.

Throughout this work, we have considered weak spatial gradient of the nutrient (see Table S1 in Ref. [18]). Even in the presence of a strong gradient our main conclusions remain valid, and we find the optimal cluster size is somewhat larger when the gradient is stronger (data shown in Fig. S5 in Ref. [18]). Although rapid spatial variation of nutrients has been shown to induce large activity fluctuations in the cell [40–43], which is expected to trigger a stronger methylation response, the ligand free energy changes by a larger amount when the cell is running through a rapidly varying nutrient profile, which shifts the trade-off point towards a larger cluster size.

V. CONCLUSIONS

In this work we have investigated the role of receptor clustering on the chemotactic efficiency of a cell. Although receptor cooperativity amplifies the cell sensitivity towards a small variation in nutrient level, the activity fluctuations inside the cell also increase since the number of clusters goes down.

Large deviation of activity from its mean value triggers a large change in methylation levels to ensure adaptation in the biochemical network. The ligand binding energy cannot keep up with such a large change in methylation energy, and the free energy difference between the active and inactive states gets controlled by methylation now. The above interplay gives rise to a performance peak at an intermediate value of the receptor cluster size.

For a noisy nutrient environment, an optimal size of the receptor signaling team was reported in earlier studies [44,45]. It was argued that receptor cooperativity amplifies not only the ligand signal, but also the noise present in it. For optimal performance, therefore, a trade-off is required where the signaling team size should be large enough for sensitive detection of small changes in ligand concentration, but small enough such that the amplified noise does not insensitize the cell response [44]. Moreover, when both ligand noise and intracellular biochemical noise are considered, the receptor clustering is beneficial as long as the amplified ligand noise stays below the biochemical noise [45]. On the other hand, we find an optimal team size even when the ligand concentration profile does not fluctuate with time, and the origin of this optimality to our best knowledge has not been reported previously.

It should be possible to test our results qualitatively in experiment. Both for a swimming cell and tethered cell we have observed the best chemotactic performance at a specific size of the receptor cluster. In our model the best performance is observed for clusters which contain ∼70 TDs. However, it may not be possible to find accurate quantitative agreement between our model and experiments. To keep our model simple and tractable, we have not considered a few aspects of the intracellular reaction network, like hexagonal geometry of the spatial arrangement of the receptor array [20,21] or, more importantly, the energy cost due to curvature of the cell membrane induced by the receptor clusters [46–48]. But our main conclusions should not get affected by these assumptions, and the interplay between ligand free energy and methylation free energy can be experimentally investigated as the cooperative interaction among the receptors is varied [11,12]. A stronger interaction among the receptors which is responsible for formation of larger clusters has been experimentally shown to induce larger activity fluctuations in a tethered cell [11,12]. Whether the variation of methylation free energy increases for stronger receptor interaction and its effect on the chemotactic efficiency $(\tau_\uparrow - \tau_\downarrow)$ [Fig. 2(b)] can be investigated in experiments. Finally, our study opens up the important question of competition between sensing and adaptation, which is relevant in a wide variety of biological systems [49–51]. It would be interesting to see if this competition gives rise to similar performance peaks in this broad class of systems as well.

ACKNOWLEDGMENTS

S.D.M. acknowledges a research fellowship [Grant No. 09/575(0122)/2019-EMR-I] from the Council of Scientific and Industrial Research (CSIR), India. S.C. acknowledges financial support from the Science and Engineering Research Board, India (Grant No. MTR/2019/000946).

[1] V. Sourjik and H. C. Berg, Receptor sensitivity in bacterial chemotaxis, Proc. Natl. Acad. Sci. USA **99**, 123 (2002).

[2] L. Turner, W. S. Ryu, and H. C. Berg, Real-time imaging of fluorescent flagellar filaments, J. Bacteriol. **182**, 2793 (2000).

[3] M. B. Elowitz, A. J. Levine, E. D. Siggia, and P. S. Swain, Stochastic gene expression in a single cell, Science **297**, 1183 (2002).

[4] A. Raj and A. Van Oudenaarden, Nature, nurture, or chance: Stochastic gene expression and its consequences, Cell **135**, 216 (2008).

[5] C. V. Rao, D. M. Wolf, and A. P. Arkin, Control, exploitation and tolerance of intracellular noise, Nature (London) **420**, 231 (2002).

[6] G. Lan and Y. Tu, Information processing in bacteria: Memory, computation, and statistical physics: A key issues review, Rep. Prog. Phys. **79**, 052601 (2016).

[7] H. C. Berg, *E. coli in Motion* (Springer Science & Business Media, Heidelberg, 2008).

[8] V. Frank, G. E. Piñas, H. Cohen, J. S. Parkinson, and A. Vaknin, Networked chemoreceptors benefit bacterial chemotaxis performance, MBio **7**, e01824 (2016).

[9] T. A. J. Duke and D. Bray, Heightened sensitivity of a lattice of membrane receptors, Proc. Natl. Acad. Sci. USA **96**, 10104 (1999).

[10] D. Bray, M. D. Levin, and C. J. Morton-Firth, Receptor clustering as a cellular mechanism to control sensitivity, Nature (London) **393**, 85 (1998).

[11] R. Colin, C. Rosazza, A. Vaknin, and V. Sourjik, Multiple sources of slow activity fluctuations in a bacterial chemosensory network, Elife **6**, e26796 (2017).

[12] J. M. Keegstra, K. Kamino, F. Anquez, M. D. Lazova, T. Emonet, and T. S. Shimizu, Phenotypic diversity and temporal variability in a bacterial signaling network revealed by single-cell fret, Elife **6**, e27455 (2017).

[13] E. Korobkova, T. Emonet, J. M. G. Vilar, T. S. Shimizu, and P. Cluzel, From molecular noise to behavioural variability in a single bacterium, Nature (London) **428**, 574 (2004).

[14] F. Matthäus, M. S. Mommer, T. Curk, and J. Dobnikar, On the origin and characteristics of noise-induced Lévy walks of *E. coli*, PloS ONE **6**, e18623 (2011).

[15] M. Flores, T. S. Shimizu, Pieter Rein ten Wolde, and F. Tostevin, Signaling Noise Enhances Chemotactic Drift of *E. Coli*, Phys. Rev. Lett. **109**, 148101 (2012).

[16] S. Dev and S. Chatterjee, Optimal methylation noise for best chemotactic performance of *E. coli*, Phys. Rev. E **97**, 032420 (2018).

[17] Y. Tu and G. Grinstein, How White Noise Generates Power-Law Switching in Bacterial Flagellar Motors, Phys. Rev. Lett. **94**, 208101 (2005).

[18] See Supplemental Material at http://link.aps.org/supplemental/10.1103/PhysRevE.103.L030401 for details of the model, simulation technique, list of parameter values, and additional data.

[19] S. Dev and S. Chatterjee, Optimal search in *E. coli* chemotaxis, Phys. Rev. E **91**, 042714 (2015).

[20] J. Liu, B. Hu, D. R. Morado, S. Jani, M. D. Manson, and W. Margolin, Molecular architecture of chemoreceptor arrays revealed by cryoelectron tomography of *Escherichia coli* minicells, Proc. Natl. Acad. Sci. **109**, E1481 (2012).

[21] A. Briegel, Xiaoxiao Li, A. M. Bilwes, K. T. Hughes, G. J. Jensen, and B. R. Crane, Bacterial chemoreceptor arrays are hexagonally packed trimers of receptor dimers networked by rings of kinase and coupling proteins, Proc. Natl. Acad. Sci. USA **109**, 3766 (2012).

[22] B. A. Mello and Y. Tu, An allosteric model for heterogeneous receptor complexes: Understanding bacterial chemotaxis responses to multiple stimuli, Proc. Natl. Acad. Sci. USA **102**, 17354 (2005).

[23] J. E. Keymer, R. G. Endres, M. Skoge, Y. Meir, and N. S. Wingreen, Chemosensing in *Escherichia coli*: Two regimes of two-state receptors, Proc. Natl. Acad. Sci. USA **103**, 1786 (2006).

[24] J. Monod, J. Wyman, and J.-P. Changeux, On the nature of allosteric transitions: A plausible model, J. Mol. Biol. **12**, 88 (1965).

[25] M. Li and G. L. Hazelbauer, Cellular stoichiometry of the components of the chemotaxis signaling complex, J. Bacteriol. **186**, 3687 (2004).

[26] S. Schulmeister, M. Ruttorf, S. Thiem, D. Kentner, D. Lebiedz, and V. Sourjik, Protein exchange dynamics at chemoreceptor clusters in *Escherichia coli*, Proc. Natl. Acad. Sci. USA **105**, 6403 (2008).

[27] H. C. Berg and P. M. Tedesco, Transient response to chemotactic stimuli in *Escherichia coli*, Proc. Natl. Acad. Sci. USA **72**, 3235 (1975).

[28] M. F. Goy, M. S. Springer, and J. Adler, Sensory transduction in *Escherichia coli*: Role of a protein methylation reaction in sensory adaptation, Proc. Natl. Acad. Sci. USA **74**, 4964 (1977).

[29] M. D. Levin, T. S. Shimizu, and D. Bray, Binding and diffusion of CheR molecules within a cluster of membrane receptors, Biophys. J. **82**, 1809 (2002).

[30] R. G. Endres and N. S. Wingreen, Precise adaptation in bacterial chemotaxis through "assistance neighborhoods," Proc. Natl. Acad. Sci. USA **103**, 13040 (2006).

[31] C. H. Hansen, R. G. Endres, and N. S. Wingreen, Chemotaxis in *Escherichia coli*: A molecular model for robust precise adaptation, PLoS Comput. Biol. **4**, e1 (2008).

[32] S.-H. Kim, W. Wang, and K. K. Kim, Dynamic and clustering model of bacterial chemotaxis receptors: Structural basis for signaling and high sensitivity, Proc. Natl. Acad. Sci. USA **99**, 11611 (2002).

[33] M. Li and G. L. Hazelbauer, Adaptational assistance in clusters of bacterial chemoreceptors, Mol. Microbiol. **56**, 1617 (2005).

[34] H. Le Moual, T. Quang, and D. E. Koshland, Methylation of the *Escherichia coli* chemotaxis receptors: Intra-and interdimer mechanisms, Biochemistry **36**, 13441 (1997).

[35] A. Celani and M. Vergassola, Bacterial strategies for chemotaxis response, Proc. Natl. Acad. Sci. USA **107**, 1391 (2010).

[36] P.-G. De Gennes, Chemotaxis: The role of internal delays, Eur. Biophys. J. **33**, 691 (2004).

[37] S. Chatterjee, R. Azeredo da Silveira, and Y. Kafri, Chemotaxis when bacteria remember: Drift versus diffusion, PLoS Comput. Biol. **7**, (2011).

[38] E. V. Pankratova, A. I. Kalyakulina, M. I. Krivonosov, S. V. Denisov, K. M. Taute, and V. Yu Zaburdaev, Chemotactic drift speed for bacterial motility pattern with two alternating turning events, PloS ONE **13**, e0190434 (2018).

[39] S. Samanta, R. Layek, S. Kar, M. K. Raj, S. Mukhopadhyay, and S. Chakraborty, Predicting *Escherichia coli*'s chemotactic drift under exponential gradient, Phys. Rev. E **96**, 032409 (2017).

[40] J. Long, S. W. Zucker, and T. Emonet, Feedback between motion and sensation provides nonlinear boost in run-and-tumble navigation, PLoS Comput. Biol. **13**, e1005429 (2017).

[41] W. Sun and M. Tang, Macroscopic limits of pathway-based kinetic models for *E. coli* chemotaxis in large gradient environments, Multiscale Model. Simul. **15**, 797 (2017).

[42] G. Micali, R. Colin, V. Sourjik, and R. G. Endres, Drift and behavior of *E. coli* cells, Biophys. J. **113**, 2321 (2017).

[43] C. Xue and X. Yang, Moment-flux models for bacterial chemotaxis in large signal gradients, J. Math. Biol. **73**, 977 (2016).

[44] R. G. Endres, O. Oleksiuk, C. H. Hansen, Y. Meir, V. Sourjik, and N. S. Wingreen, Variable sizes of *Escherichia coli* chemoreceptor signaling teams, Mol. Syst. Biol. **4**, 211 (2008).

[45] G. Aquino, D. Clausznitzer, S. Tollis, and R. G. Endres, Optimal receptor-cluster size determined by intrinsic and extrinsic noise, Phys. Rev. E **83**, 021914 (2011).

[46] R. G. Endres, Polar chemoreceptor clustering by coupled trimers of dimers, Biophys. J. **96**, 453 (2009).

[47] C. A. Haselwandter and N. S. Wingreen, The role of membrane-mediated interactions in the assembly and architecture of chemoreceptor lattices, PLoS Comput. Biol. **10**, e1003932 (2014).

[48] W. Draper and J. Liphardt, Origins of chemoreceptor curvature sorting in *Escherichia coli*, Nat. Commun. **8**, 1 (2017).

[49] S. Gepshtein, L. A. Lesmes, and T. D. Albright, Sensory adaptation as optimal resource allocation, Proc. Natl. Acad. Sci. USA **110**, 4368 (2013).

[50] S. G. Solomon and A. Kohn, Moving sensory adaptation beyond suppressive effects in single neurons, Curr. Biol. **24**, R1012 (2014).

[51] B. Wark, B. N. Lundstrom, and A. Fairhall, Sensory adaptation, Curr. Opin. Neurobiol. **17**, 423 (2007).